Light Scattering Studies on Polyelectrolyte Complexes

Herbert Dautzenberg,

Max-Planck-Institute of Colloids and Interfaces,

D-14476 Golm, Am Mühlenberg, Germany

Abstract: The Coulomb interaction between oppositely charged polyelectrolytes leads to spontaneous formation of interpolymer complexes. Such complexes are of high practical relevance, but also interesting objects of fundamental research. The level of aggregation depends on the nature of the components as well as on the medium and external conditions of the polyelectrolyte complex formation. An appropriate combination of methods provides detailed information on the stoichiometry and structure of such systems. Especially, light scattering techniques proved to be a powerful tool in studying the structure and behavior of the complexes in solution. Selected examples will demonstrate the efficiency of such investigations.

Introduction

One of the interesting features of polyelectrolytes is their ability to form stable interpolymer complexes between oppositely charged species, due to a cooperative, attractive Coulomb interaction. Such complexes are of high practical relevance from industrial applications as flocculants, coatings and binders up to biological and medical purposes.

The mixing of solutions of polyanions and polycations leads to spontaneous aggregation under release of the counterions.

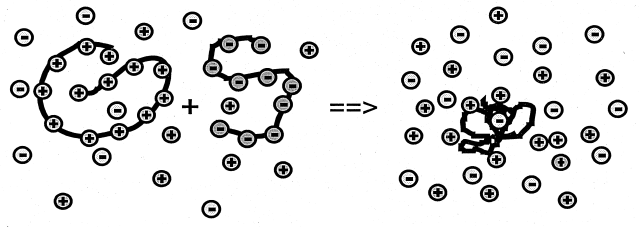

Fig. 1: Scheme of polyelectrolyte complex formation.

This reaction can be described by the following equation:

$(>\!-A^- c^+)_n + (>\!-C^+ a^-)_m \;<===>$

$(>\!-A^- C^+)_x + (>\!-A^- c^+)_{n-x} + (>\!-C^+ a^-)_{m-x} + x\,a^- + x\,c^+$

where A^-, C^+ - are the charged groups of the polyelectrolytes, a^- , c^+ - counterions,

n , m - number of the anionic and cationic groups in solution,

$\theta = x/n$, $n<m$ or $\theta = x/m$, $m<n$, θ - degree of conversion, $n/m = X$ – molar mixing ratio.

 CCC 1022-1360/00/$ 17.50+.50/0

As borderline cases for the resulting structures of polyelectrolyte complexes (PEC) two models are discussed in the literature:

- the ladder-like structure, where complex formation takes place on a molecular level via conformational adaptation
- and the scrambled egg model, where a high number of chains are incorporated into a particle.

PEC formation between polyions with weak ionic groups and significantly different molecular weights in non-stoichiometric systems results in soluble complexes, which are structured according to the ladder model, consisting of hydrophilic single-stranded and hydrophobic double-stranded segments. Such systems were comprehensively studied by the groups of Tsuchida[1,2] and Kabanov[3,4]. Stop flow measurements[5] showed that PEC formation takes place in less than 5 μs, nearly corresponding to the diffusion collision of the polyion coils. In salt-free solutions frozen structures in a non-equilibrium state are formed. The presence of small amounts of salt enables rearrangement and exchange processes yielding PECs in thermodynamic equilibrium.

However, in most applications PEC formation is carried out under conditions, which lead to highly aggregated systems (scrambled egg model), often to macroscopic flocculation. Complex formation between polyanions and polycations with strong ionic groups and/or comparable high molecular weight results in such structures. Because of the high cooperativity of the ionic binding PEC formation takes place far from the thermodynamic equilibrium, even in the presence of salt. The degree of aggregation is mainly controlled by the concentration of the component solutions. In highly diluted solutions ($<10^{-4}$ g/ml) quasi-soluble particles on a colloidal level are formed, which can be studied by all methods, normally used in polymer characterization.

The main interest of our work was focused on the stoichiometry of the ionic binding, the overall composition and the structure of the PEC particles. A general problem consists in the huge variety of parameters, which may influence the course of PEC formation. The macromolecular characteristics of the components, the medium conditions as well as the external mixing parameters must be taken into account. Many investigations are necessary to recognize the general tendencies, because the superposition of several effects leads to a high individuality of the structure and behavior of the PEC particles [6].

Experimental

Materials

Results reported here were mainly obtained using commercial standards (Polymer Standard Service, Mainz, Germany) of sodium poly(styrene sulfonate) (NaPSS-xt, where x denotes the molecular weight in kDalton)) and poly(methacrylate) (NaPMA, M_w = 114 000 g/mol) as polyanions and poly(diallyldimethylammonium chloride) (PDADMAC, M_w = 250 000 g/mol) and its copolymers (COPx, where x corresponds to the mol% of DADMAC) with acrylamide of various compositions[7] as polycations. Additionally, some findings will be given about PECs between ionically modified poly(N-isopropylacrylamide) (PNIPAM) samples AIFL2 (polycation) and AIFL3 (polyanion) with about 10 mol% of ionic groups. For details of synthesis and characterization see[8].

All samples were carefully dialyzed and freeze dried. As solvents deionized water or NaCl solutions in the neutral pH-range were employed.

Preparation of PECs

For the light scattering studies PEC formation was carried out directly in the scattering cell of the Sofica instrument. As standard condition 10 mL of one component of a monomolar concentration of $2.5 \cdot 10^{-4}$ mol/L were put into the cell and the counterpart solutions of twice of the molar concentration were added up to the desired mixing ratio X. The dosage was carried out continuously with a slow rate of 4 mL/h under gentle stirring at 22 °C. Solutions were made dustfree by filtration through 0.45 µm membrane filters of cellulose nitrate (Sartorius, Germany). In the case of subsequent addition of salt after the preparation of the PECs the volume in the scattering cell was reduced to 10 mL. Then a 2 N NaCl solution was added in small steps. The scattering curves were recorded after each step of dosage. The concentrations and the refractive index increments of the PECs were calculated assuming a 1:1 stoichiometry of ionic binding.

Methods

An appropriate combination of methods provides comprehensive information about the stoichiometry and structure of the PEC particles. The methods used are collected together with the data about the instruments and the resulting information in Table 1.

Table 1. Methods used in PEC characterization

Method	Instrument	Information
UV/VIS spectroscopy	Lambda 2, Perkin Elmer	Stoichiometry of ionic binding
Potentiometry	Ionmeter, Metrom	Release of counterions
Ultracentrifugation	AUC, Beckman, Palo Alto	Overall composition
Viscometry	Viscoboy, Lauda, Ubbelohde, Schott	Overall composition, degree of swelling
Static light scattering	Sofica 42 000 Wippler/Scheibling	Particle mass, size and structural density
Dynamic light scattering	Simultan, ALV Langen	Hydrodynamic radius
Electron microscopy	EM 102, Siemens	Structure type, size
X-ray microscopy	Microscope: Univ. Göttingen, X-ray source: Bessy, Berlin	Structure type, size, density profile

Light scattering, in particular, proved to be a powerful tool in studying the structure and behavior of highly aggregated PEC particles. The size of the investigated PECs ranged up to several 100 nm, leading to a strong angular dependence of the scattering curves. On the one hand, this causes problems in the extrapolation procedure to zero scattering angle. On the other hand, the shape of the scattering curve contains more information than used in determining the particle mass and radius of gyration. To solve these problems we developed an improved algorithm of data analysis, basing on a comparison of the experimental scattering curves with theoretically calculated ones for various basic structure types[9]. This procedure should be briefly described in the following.

Algorithm of Light Scattering Data Analysis

Static Light Scattering

For highly diluted systems of compact particles interparticular interferences can be neglected and the Rayleigh ratio **R(q)** of the scattering intensity is given by the simple expression:

$$\mathbf{R(q) = K\, c\, M_w\, P_z(q)} \qquad (1)$$

where **K** is a contrast factor, containing the optical parameters of the system, **c** - mass concentration in g/ml, $\mathbf{M_w}$ - weight average of the molecular mass of the scattering particles,

$P_z(q)$ - z-average of the intraparticular scattering function, $q = (4\pi/\lambda) \sin \Theta/2$, λ– wave length in the medium, Θ - scattering angle between the incident and the scattered beam. Describing the polydispersity of the particle system by a continuous normalized mass distribution function $p_w(M)$, one obtains:

$$M_w = \int_0^\infty M\, p_w(M)\, dM \tag{2}$$

$$P_z(q) = (1/M_w) \int_0^\infty P(q,M)\, M\, p_w(M)\, dM \tag{3}$$

In the framework of the Rayleigh-Debye-Approximation (RDA) the relation

$$P_z(q) = 1 - (1/3) \left\langle S^2 \right\rangle_z q^2 + \ldots \tag{4}$$

was derived, whatever the shape and the structure of the particles, where $\left\langle S^2 \right\rangle_z$ is the z-average of the square of the radius of gyration.

For particle sizes smaller than 50 nm the scattering curves can be analyzed by a Zimm plot ($K\,c/\,R(q)$ versus q^2) or a Guinier plot ($\ln R(q)/\,K\,c$ versus q^2), providing by extrapolation to the scattering angle zero, M_w and $\left\langle S^2 \right\rangle_z$ without any assumptions. However, no conclusions can be drawn from the scattering curve about the structure and polydispersity of the particle system. Because the scattering functions of various structure models are known in the RDA (justified for PEC particles due to the swollen structures), $P_z(q)$ can be calculated, assuming the type of the distribution function $p_w(M)$.

In the following we restrict the considerations to the model of polydisperse systems of homogeneous spheres, which has been proved quite well in describing the scattering curves of the PEC solutions investigated and could also be confirmed by electron microscopy. As distribution function we used a special logarithmic distribution of radii with the size parameter a_m and the polydispersity σ_a:

$$p_w(a) = \frac{a^{-5/2} \exp(-(\ln a - \ln a_m)^2 / 2\sigma_a^2)}{\sqrt{2\pi}\sigma_a a_m^{-3/2} \exp(9\sigma_a^2/8)} \tag{5}$$

This distribution function manages that M_w becomes independent of σ_a:

$$M_w = (4\pi/3)\, \rho\, N_A\, a_m^3 \tag{6}$$

where N_A - Avogadro's number and ρ is the average polymer density in the particle, the reciprocal of the degree of swelling. The radius of gyration is given by:

$$\left\langle S^2 \right\rangle_z = \frac{3}{5} a_m{}^2 e^{5\sigma_a^2} \tag{7}$$

The parameter σ_a corresponds for low polydispersities to the relative standard deviation. The choice of the type of distribution function is of minor importance as it is demonstrated in the following section.

The intraparticular scattering function of spheres with the radius **a** is given as[10]:

$$P(q) = \left(3 \frac{\sin aq - aq \cos aq}{a^3 q^3} \right)^2 \tag{8}$$

Because **R(q)** is proportional to M_w and **P(q)** depends in the RDA on the product **q** times **a**, changes in mass and size correspond in a scaled, double logarithmic plot to axis parallel shifts. Therefore, model calculations yield in such a plot for each structure model a set of master curves with different polydispersities. As shown in a previous paper[11] the structure type can be well estimated, if an appropriate section of the scattering curve is known. From the assignment of an experimental curve to an appropriate theoretical one also the polydispersity can be determined. The position of the experimental on the fitting curve yields M_w and a_m as well as ρ according to equation (6).

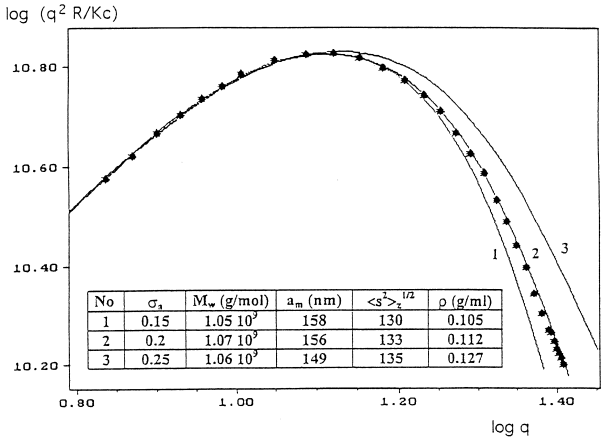

No	σ_a	M_w (g/mol)	a_m (nm)	$\langle s^2 \rangle_z^{1/2}$	ρ (g/ml)
1	0.15	$1.05\ 10^9$	158	130	0.105
2	0.2	$1.07\ 10^9$	156	133	0.112
3	0.25	$1.06\ 10^9$	149	135	0.127

Fig.2: Scattering curve of a PEC between anionically and cationically modified PNIPAM (symbols) and its interpretation by theoretical curves of polydisperse systems of spheres of different polydispersity (see the Table in Fig. 2).

By a plot **log (q^k R(q))** versus **log q** with an appropriate **k**-value it can be achieved that the scattering curve passes through a maximum, where its width depends sensitively on the polydispersity. Therefore, σ_a can be obtained with an accuracy better than 0.05 and the structural parameters with an error in the range of 1 %.

Remarks about the Mass Distribution Function

In the following we compare the logarithmic distribution function with the Schulz-Zimm (Γ-) distribution, which is often used to describe the polydispersity of polymers.

The Schulz-Zimm (Γ-) distribution is given by the expression:

$$p_W(M) = \frac{((z+1)/M_W)^{z+1}}{\Gamma(z+1)} M^z \, e^{-(z+1)M/M_W} \tag{9}$$

One can calculate all moments of this distribution by the integration rule:

$$\int_0^\infty e^{-qx} \, x^{p-1} \, dx = q^{-p} \, \Gamma(p) \tag{10}$$

It is easy to show that:

$$z = (M_w/M_n - 1)^{-1} \tag{11}$$

The case $z = 0$ represents the borderline of highest polydispersity.

To estimate the influence of the polydispersity on the quantities provided by light scattering, we calculated for the model of spheres the z-average of the square of the radius (static light scattering) and the hydrodynamic radius via the Einstein-Stokes relation from the z-average of the diffusion coefficient (dynamic light scattering) in relation to the radius a_m (defined by equation (6)):

$$\langle a^2 \rangle_z / a_m^2 = (z+1)^{-5/3} \, \Gamma(z+8/3)/\Gamma(z+1) \tag{12}$$

$$= 1.504 \quad (z = 0)$$

$$R_h^{app}(q=0) = a_m (z+1)^{2/3} \frac{\Gamma(z+1)}{\Gamma(z+5/3)} \quad = 1.107 \, a_m \quad (z=0) \tag{13}$$

From (12) and(13) it follows for the maximum of the structure sensitive parameter for z = 0:

$$\langle s^2 \rangle_z^{1/2} / R_h^{app}(q=0) = 1.108 * 0.775 = 0.859 \tag{14}$$

The polydispersity described by the Schulz-Zimm-distribution causes only small changes of these quantities.

Quite different effects result from the logarithmic distribution function

$$p_W(M) = \frac{M^{-3/2} \exp(-(\ln M - \ln M_W)^2 / (2\sigma_M^2))}{\sqrt{2\pi}\sigma_M M_w^{-1/2} \exp(\sigma_M^2/8)} \tag{15}$$

where $\sigma_M = 3 \, \sigma_a$.

By the integration rule:

$$\int_0^\infty x^i p_W^j(x) dx = x_j^i \exp((2ij + i^2 + 2i)\sigma_j^2/2) \tag{16}$$

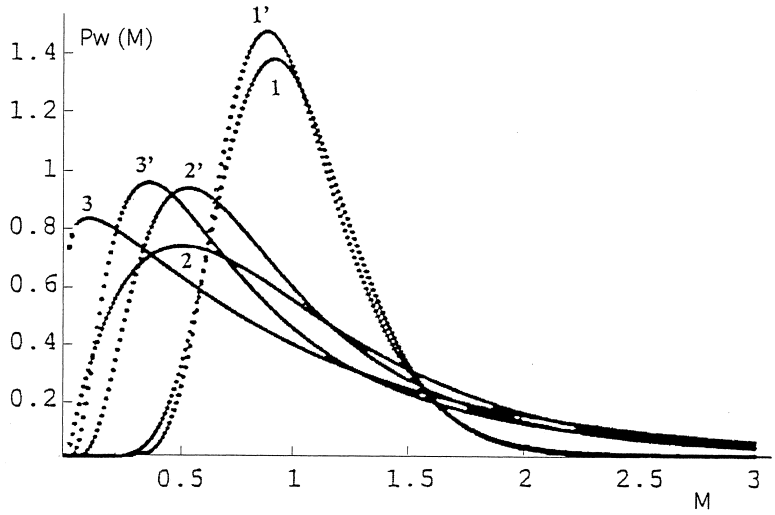

Fig. 3: Comparison of the Schulz-Zimm and the logarithmic distribution function at the same M_w and $\langle s^2 \rangle_z$ values for spheres: Schulz-Zimm: 1 – z = 10, M_w/M_n = 1.1, 2 – z = 1, M_w/M_n = 2, 3 – z = 0.1, M_w/M_n = 11, logarithmic distribution: 1' - σ_a = 0.296, M_w/M_n = 1.09, 2' - σ_a = 0.649, M_w/M_n = 1.52, 3' - σ_a = 0.827, M_w/M_n = 1.98

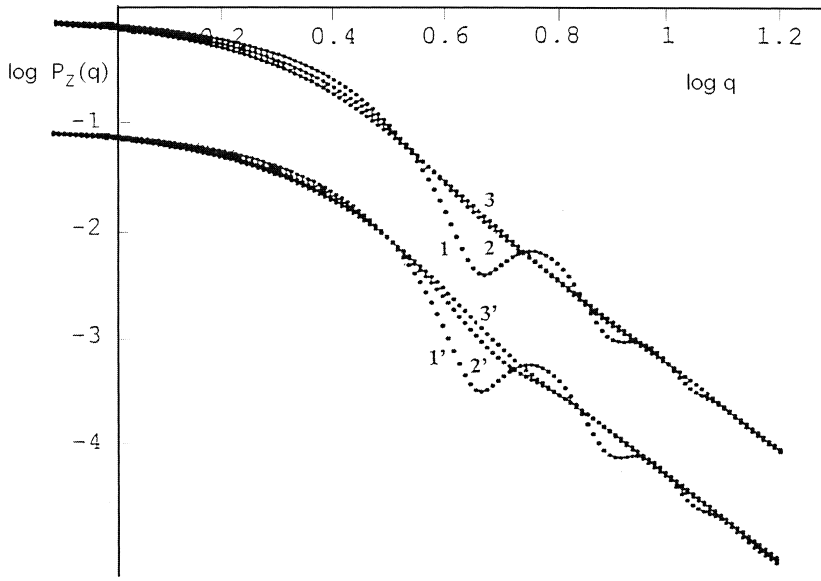

Fig. 4: Scaled double logarithmic plot of P_z (q) for the distribution functions of Fig. 3. To avoid overlapping the curves for the logarithmic distributions are shifted down by 1 unit.

it follows: $M_w/M_n = \exp(\sigma_M^2)$ (17)

$$\langle a^2\rangle_z / a_m^2 = \exp(5\sigma_M^2/9) \quad (18)$$

$$R_h^{app}(q=0) = a_m \exp(\sigma_M^2/9) \quad (19)$$

and $$\langle s^2\rangle_z^{1/2} / R_h^{app}(q=0) = \exp(\sigma_M^2/6) * 0.775 \quad (20)$$

For the same M_w/M_n ratios the polydispersity has a much higher (and unlimited) effect on the radii for the logarithmic distribution function.

Fig. 3 reveals the reason of the different behavior of the distribution functions. While for the Schulz-Zimm-distribution higher $\langle s^2\rangle_z$ –values at fixed M_w are realized by adding a great amount of small particles, for the logarithmic distribution the long tail is responsible for this.

In Fig. 4 the scattering curves obtained with the distribution functions of Fig. 3 are compared. There is nearly no difference between the curves with the same M_w and $\langle s^2\rangle_z$. Therefore, independent of the choice of the distribution function we get from the scattering curves the same values of the structural parameters. However, it must be noticed that the conclusions on M_w/M_n depend strongly on the type of the distribution function.

Dynamic Light Scattering

Dynamic light scattering measurements yield the electric field correlation function $g(q,t)$, which can be expressed for a polydisperse system of particles as (see [12,13]) :

$$g(q,t) = \int_0^\infty G(q,\Gamma) e^{-\Gamma t} d\Gamma \quad (21)$$

where Γ is the decay constant or line width and $G(q,\Gamma)$ is the normalized distribution of Γ measured at a fixed value of q. Considering the center of mass motion of particles, Γ is given by: $$\Gamma = D q^2 \quad (22)$$

where D is the translational diffusion coefficient. The correlation function (21) can be analyzed by an inverse Laplace transform (Provencher[14]), providing the distribution function of Γ, or by a series expansion of $\ln g(q,t)$ and a cumulant fit. For polydisperse systems the first cumulant represents the z-average of the diffusion coefficient. At finite concentrations and q-values an apparent diffusion coefficient is obtained. Because of the high dilution of the PEC solutions, the concentration dependence of D_{app} may be neglected. For compact, nearly spherical particles the angular dependence is mainly caused by the polydispersity and can be written as:

$$D_{app}(q) = \frac{\int_0^\infty D(M)P(q,M)Mp_w(M)dM}{\int_0^\infty P(q,M)Mp_w(M)dM} \quad (23)$$

Using the Einstein-Stokes-equation $R_H = \frac{kT}{6\pi\eta D}$ one obtains:

$$R_H{}^{app}(q) = \frac{\int_0^\infty a^3 P(q,a)\, p_w(a)da}{\int_0^\infty a^2 P(q,a)\, p_w(a)da} \quad (24)$$

A comparison[15] of the angular dependence of $R_H^{app}(q)$ and of $P_z(q)$ with regard to the polydispersity shows an opposite behavior. While the curves of $P_z(q)$ become flatter with rising polydispersity, the angular dependence of $R_H^{app}(q)$ increases. Therefore, the combination of static and dynamic light scattering provides a reliable information about the polydispersity of the systems under study.

Results and Discussion

Stoichiometry of Ionic Binding

The first point in judging the composition of the PEC particles is the determination of the stoichiometry of the ionic binding, i.e. of the degree of conversion. For the UV-active polyanion NaPSS this could be done by spectroscopy[16]. The binding of NaPSS in a complex causes a slight shift in the spectrum, which leads to clearly pronounced peaks in the difference spectra of the PEC solution and a NaPSS solution of the same polyanion concentration. The height of the peaks is strongly correlated to the mixing ratio and could be used to determine the degree of conversion.

The experimental findings showed that the component in deficiency is completely bound into the complex, corresponding to a 1:1 stoichiometry.

In the case of non-UV-active components colloid titration[17] with an ionic dye as indicator can be used to determine the stoichiometry. The binding of the cationic dye toluidine blue by a polyanion causes a clearly pronounced shift in the spectrum. Since the complex binding of a polycation is absolutely favored in comparison to the low molecular dye, the onset of the shift indicates the full consumption of the polycation, allowing an exact determination of the stoichiometry of binding.

We found for all PECs between polyelectrolytes with strong ionic groups a 1:1 stoichiometry, even for the DADMAC-acrylamide copolymers with low content of ionic groups, i.e. a strong mismatching of the charge distances of the components.

Potentiometry with a Cl^- sensitive electrode allows estimating the release of the counterions. Due to the counterion condensation (Manning[18]), the counterions of a highly charged polyelectrolyte have a remarkable reduced activity. The binding of the ionic groups of the polyelectrolytes during PEC formation leads to a corresponding release of the counterions.

While pure polycation solutions showed this reduced activity, the addition of a polycation to a NaPSS solution resulted in an activity coefficient of 1 compared with NaCl solutions. At the 1:1 mixing ratio a break point occurred. These results monitor the full release of the counterions and confirm the 1:1 stoichiometry of ionic binding.

Overall Composition of the PEC Particles

Although a 1:1 stoichiometry of ionic binding was found for nearly all studied systems, the major component can be incorporated in excess in the complex. In salt-free systems this question can be answered by viscometric studies. According to Einstein's law, the viscosity of a suspension of particles is proportional to the reciprocal of their density. PEC formation causes two dominating effects: the transition of the bound polyelectrolyte chains to a much more compact conformation and the decrease of the viscosity of the free excess component due to the release of the counterions and the increase of the ionic strength of the medium.

The minimum in the dependence of the viscosity on mixing ratio X corresponds to the 1:1 mixing ratio. From the viscosity at this point the structural density of the PEC can be estimated. The viscosity at lower mixing ratios results from the contributions of the complex and the free excess component. A quantitative analysis[19] of the viscosity data yields the amount of the free excess polyelectrolyte and from that the overall stoichiometry of the complex. For all PECs increasing excess binding (up to a factor 1.5) of the major component with decreasing mixing ratio was found.

For the UV-active NaPSS also analytical ultracentrifugation with UV-detection can be employed to determine the content of NaPSS in the PEC from the absorption level of the PEC solution and the supernatant[20].

The obtained stoichiometric factor is somewhat higher than that from viscometry. This may be understood by the fact that viscometry monitors only the chains which underwent a transition to a compact structure as incorporated in the PEC, while ultracentrifugation also loosely attached ones includes. The excess binding of the major component explains the colloidal sta-

bility of the PEC solutions. Obviously, these excess chains form a charged, electrostatically stabilizing shell around the neutralized core of a PEC particle.

Structure of the PEC Particles

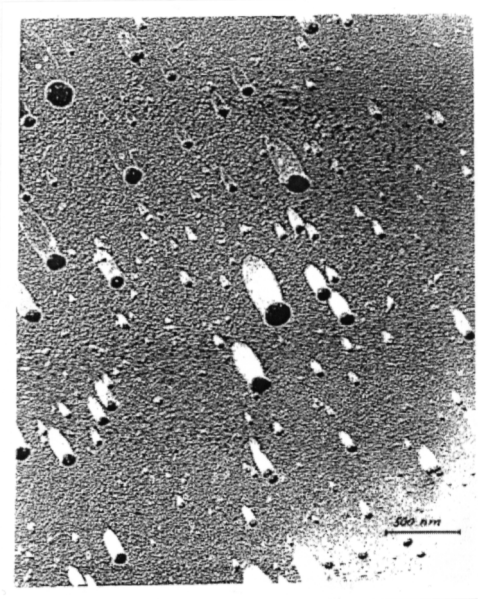

Fig. 5: Electron micrograph of the PEC PDADMAC/NaPSS-66t, $c_c = 2\ 10^{-4}$ g/mL, X = 0.8.

Microscopic Studies

Imaging techniques are the best way to get an impression of the structure of particles. We used electron microscopy and X-ray absorption microscopy for this purpose.

To avoid artefacts, cryo-preparation was used for the electron micrographs*. Fig. 5 shows that the PECs exist as highly polydisperse systems of nearly spherical particles. X-ray absorption microscopy at the absorption edge of oxygen allows to study the structures directly in water[21]. Such micrographs* fully confirmed the findings of electron microscopy. Additionally, we got an information about the density profile of the particles, indicating nearly homogeneous spheres.

Light Scattering Studies

Knowing the structure type of the PEC particles, a detailed analysis of the light scattering data according to the above-described algorithm provides comprehensive information about the structural characteristics. So the effect of different parameters on the structure and behavior of PECs could be studied: mixing ratio, polymer concentration, molecular weight and charge density of the polyelectrolytes, ionic strength during complex formation, subsequent addition of salt, and temperature behavior of PECs between temperature-sensitive polyelectrolytes.

---

* We thank Dr. Tesche (Fritz-Haber-Institute, Berlin) and Dr. Thieme (University of Göttingen) for their support in carrying out the electron and X-ray microscopic investigations.

Selected results will be presented here, demonstrating the high efficiency of light scattering techniques.

Mixing Ratio

The effect of the mixing ratio on the structural parameters of the PECs depends strongly on the components used. For highly charged, strong polyelectrolytes only slight changes of the shape of the scattering functions were found. For complexes between NaPSS-66t and PDADMAC the scattering curves could be fitted quite well by polydisperse systems of spheres with σ_a = 0.5 - 0.6. The resulting structural parameters for PECs prepared in pure water and in 0.01 N NaCl solution are given in Fig. 6.

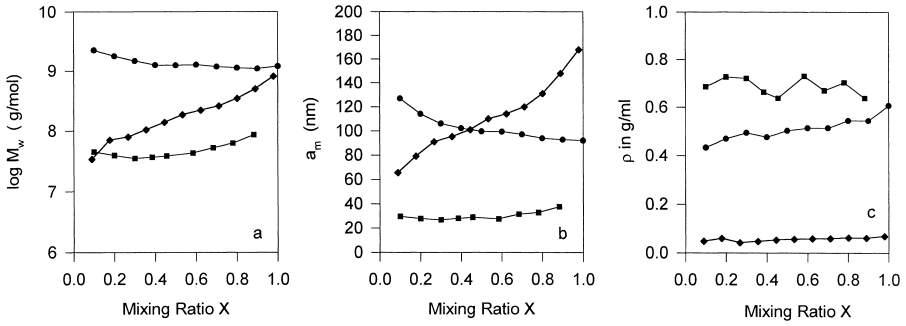

Fig. 6: Structural parameters of various complexes as function of the mixing ratio: ● - NaPSS-66t/PDADMAC in water, ■ - NaPSS-66t/PDADMAC in 0.01 N NaCl, ◆ - AIFL3/AIFL2 in 0.01 N NaCl.

Ignoring the effect of polydispersity would provide the structural density (calculated from $\mathbf{M_w}$ and the z-average of the square of the radius) by a factor 15 to low. In pure water the particle mass and size decrease slightly with rising X, while the density increases somewhat. In 0.01 N NaCl a much lower level of aggregation, but slight increase with rising mixing ratio were observed. The structural density remained nearly constant. Therefore, in both cases the formation of new particles and not their further growth is the dominating process. The lower level of aggregation at low ionic strength is obviously caused by a screening of the Coulomb interaction, which enables rearrangement and exchange processes, as it is well known from soluble complexes. In pure water nearly all PEC systems under study showed a similar behavior. In contrast to that, we observed a strong increase in particle mass and size with increasing X for PECs between ionically modified PNIPAM samples with low contents of ionic groups during complex formation in 0.01 N NaCl.

Polyelectrolyte Concentration

For the system NaPSS-66t/PDADMAC we studied the PEC formation in a broad range of concentration of the component solutions (c_c = 1 10^{-5}, 2 10^{-5}, 5 10^{-5}, 1 10^{-4}, 2 10^{-4}, 5 10^{-4}, 1 10^{-3} g/mL (see[15])). At each concentration PECs were prepared up to X = 0.5 and for the higher concentrations the PEC solutions were diluted in an appropriate manner for the light scattering measurements. The analysis of the scattering curves yielded the mass and size given in Fig. 7.

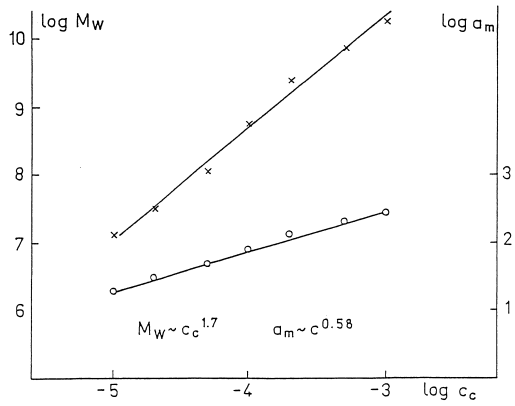

Fig. 7: Structural parameters M_w and a_m of the PEC NaPSS-66t/PDADMAC in dependence on the polycation concentration (from Ref. 15).

Fig. 7 shows that simple power laws were obtained for the concentration dependence of the mass and size of the PEC particles, the exponent of which corresponds to $M_w \sim a_m^3$, the expected relation for homogeneous spheres.

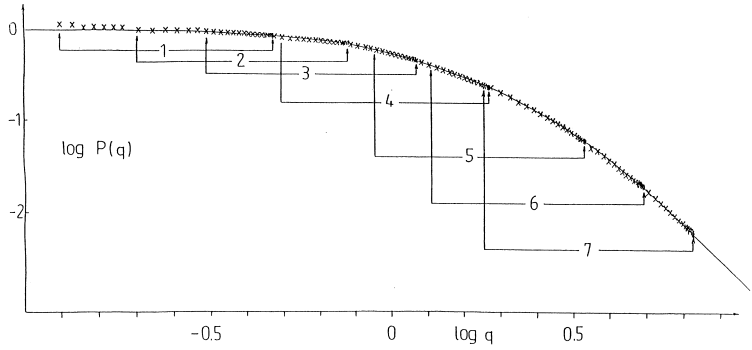

Fig. 8: Superposition of the normalized scattering curves of the PECs NaPSS-66t/PDADMAC at different concentrations, crosses – experimental points, full line – model curve with σ_a = 0.6 (from Ref. 15).

The structural density of the PECs is ρ = 0.43 g/mL. Because all scattering curves could be fitted by systems of spheres with the same polydipersity, the normalized curves give a common one, reaching up to the asymptotic q^{-4} – range of spheres (Fig. 8).

The results of static light scattering could be confirmed by dynamic light scattering. Fig. 9 depicts the angular dependence of the apparent hydrodynamic radius of the same systems as above in comparison to the theoretically calculated curves according to equation (24), using the parameters obtained by static light scattering. The agreement is quite acceptable, taking into account the necessary assumptions and simplifications.

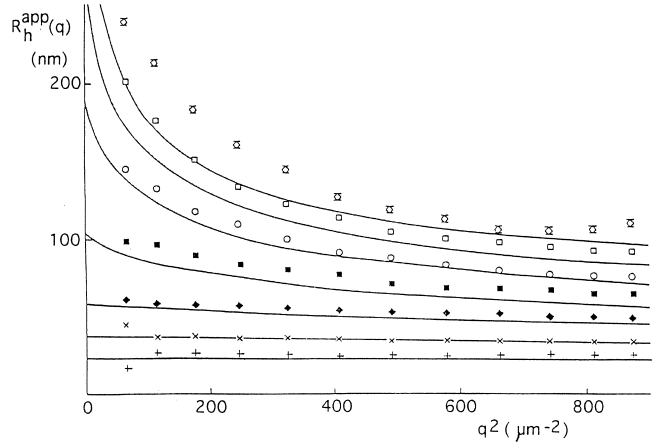

Fig. 9: Angular dependence of the apparent hydrodynamic radius of the PECs NaPSS-66t/PDADMAC at different concentrations, symbols – experimental points, full lines – model curves (from Ref. 15).

Summarizing we can state that the light scattering experiments lead to the same structure model as revealed by microscopic methods. The model of polydisperse systems of homogeneous spheres is confirmed by four facts.

- exact fits of the static light scattering curves,
- the expected $M \sim a^3$ – dependence for PEC "homologues" prepared at different polymer concentrations,
- the asymptotic q^{-4} behavior of compact spheres,
- and the agreement between the results of static and dynamic light scattering under the assumption of polydisperse systems of spheres.

PEC Formation in the Presence of Salt

To judge the effect of the presence of salt more in detail we studied the complex formation between NaPSS and PDADMAC up to an ionic strength of 0.2 N NaCl. The characterization of PECs prepared at various contents of NaCl[22] revealed a clearly pronounced minimum in the dependence of the particle mass and size on the ionic strength (Fig. 10), while the structural density remained nearly constant.

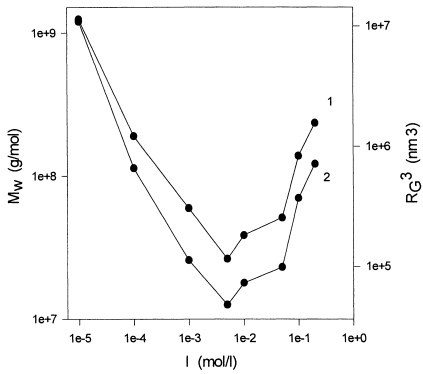

Fig. 10: Particle mass (1) and size (2) of the PEC NaPSS-66t/PDADMAC (X=0.5) as function of the ionic strength.

The decrease of the level of aggregation at low ionic strengths may be understood by a favoring of the formation of ionic bindings due to a conformational adaptation of the polyelectrolyte chains. The increase at higher ionic strength is probably caused by secondary aggregation induced by the presence of salt. In comparison to salt-free systems the level of aggregation in the minimum is reduced by nearly two orders of magnitude. This opens a second way to control the mass of the PEC particles

Subsequent Addition of Salt

For practical uses the response of PECs to a subsequent change of the ionic strength of the medium is an important question. Depending on the nature of the components two different effects govern the behavior of the PEC systems, secondary aggregation and dissolution.

Complexes between NaPSS and PDADMAC are stable with regard to the ionic binding up to ionic strengths of a few mol/L[23]. Addition of NaCl caused only secondary aggregation and macroscopic flocculation, as demonstrated in Fig. 11.

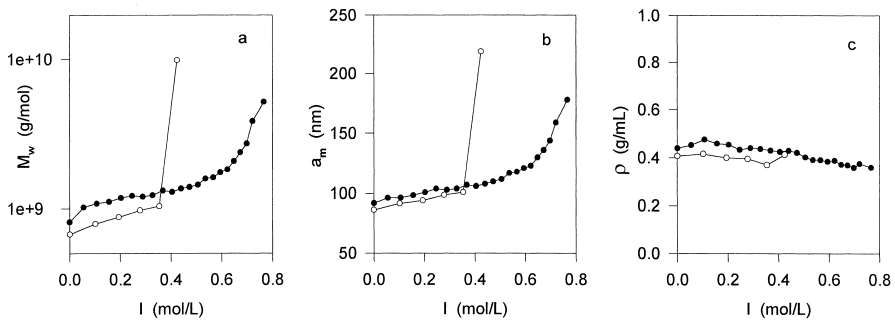

Fig. 11: Ionic strength dependence of the structural parameters of the complex PDADMAC/ NaPSS during subsequent addition of NaCl: a - particle mass, b - particle radius, c - structural density, ●- X = 0.3, o - X = 0.6 (from Ref. 23).

At higher mixing ratio secondary aggregation is much stronger pronounced and macroscopic flocculation occurred at lower ionic strength. Obviously, the salt screens the charges of the stabilizing shell, the thickness of which decreases with rising X. Interestingly, the structural density remained constant. A different behavior was found for complexes with Na-PMA as

polyanion. The particle mass increased only slightly with rising ionic strength, whereas the particle radius increased strongly, indicating a high swelling of the particles. Complete dissolution occurred at a critical salt concentration of 0.6 N.

PECs of Temperature-sensitive Polyelectrolytes

The neutral, water-soluble polymer PNIPAM has a lower critical solution temperature of about 34 °C. An introduction of ionic groups by copolymerization of NIPAM leads to changes of the transition temperature or to a complete loss of the phase transition[8]. Complex formation between such components offers the chance to restore the temperature dependence and to prepare temperature-sensitive gels on a nm-scale. To check this, we prepared PECs between a cationically (AIFL 2) and an anionically (AIFL 3) modified PNIPAM sample and studied their temperature behavior.

Fig. 12 shows a selection of scattering curves obtained between 25 and 50 °C in 0.01 N NaCl. With rising temperature only a small increase of the scattering level was observed, indicating a slight additional aggregation. But simultaneously, the angular dependence decreases significantly. Both effects are reversible.

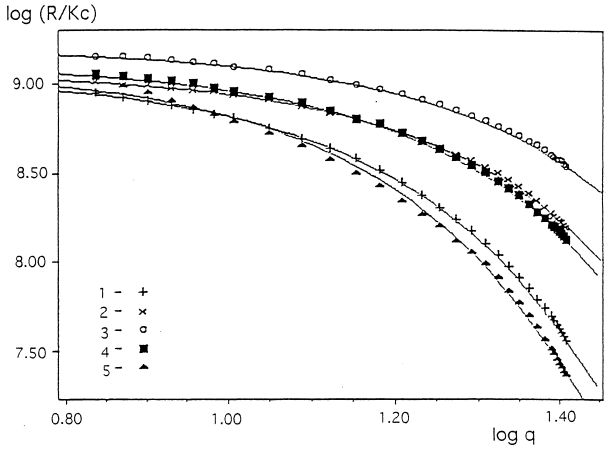

Fig. 12: Selected scattering curves of the PEC AIFL2/AIFL3 in 0.01 N NaCl at different temperatures: 1 – 25, 2 – 35, 3 – 50, 4 – 35, 5 – 25 °C.

All curves could be fitted in an excellent manner by relatively monodisperse systems of spheres with $\sigma_a = 0.2$. The changes in mass and size of the PEC result in a strong variation of the structural density, which is fully reversible. Such complexes may be potential candidates for temperature-controlled delivery systems of drugs.

From the point of view of the efficiency of static light scattering the temperature behavior of the PEC AIFL2/AIFL3 at higher ionic strength of 0.025 N NaCl is very interesting. Higher ionic strengths encourage the aggregation tendency with rising temperature.

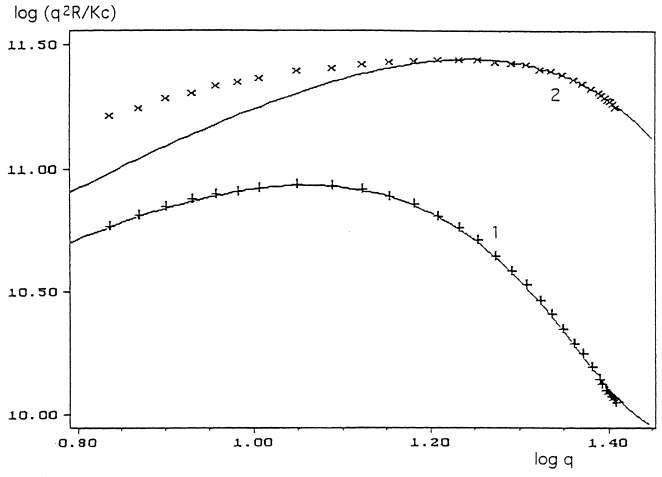

Fig. 13a: Scattering curves of the PEC AIFL2/AIFL3 in 0.025 N NaCl at 25 (1) and 50 (2) °C.

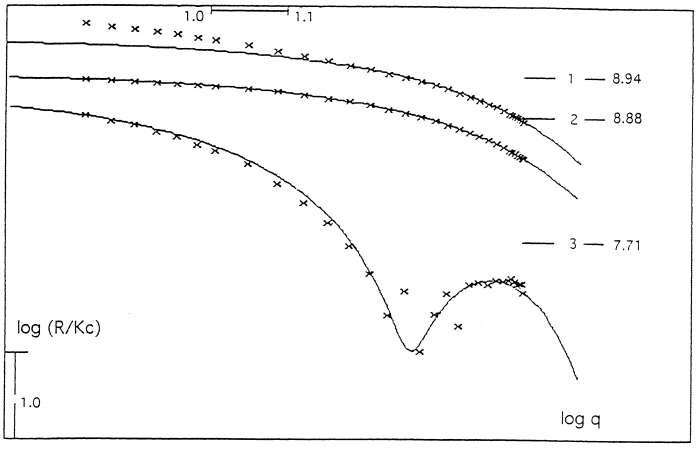

Fig. 13b: Curve separation, starting from the wide-angle range, 1 - original curve, 2 - fit curve of the wide-angle range, 3 - difference curve.

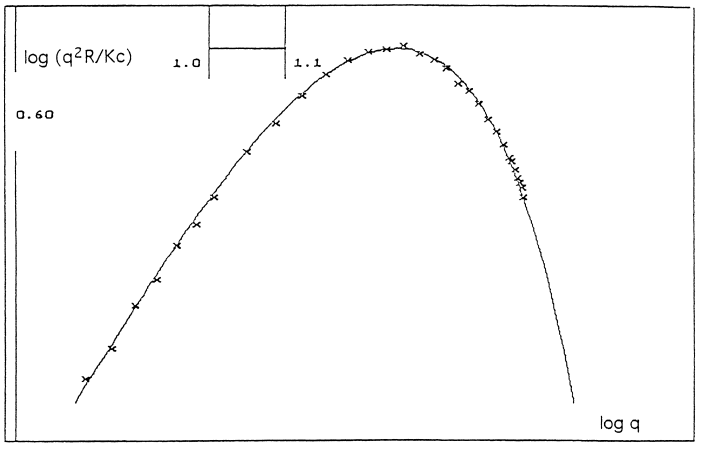

Fig. 13c: Symbols: Original curve minus theoretical curve 3 of (b), full line: Curve fit (parameters see Table 2).

While the scattering curve at 25 °C in Fig. 13a corresponds to a system of spheres with σ_a = 0.2, only the wide-angle range of the scattering curve at 50 °C could be fitted by this model. The higher scattering values at smaller scattering angles in comparison to the model curve clearly indicate the generation of a larger component. Therefore, we made an attempt to separate both components by an iterative procedure. At first we determined from the wide-angle range the parameters of the major component and calculated its contribution in the whole range (Fig. 13b, curve 2)). The difference curve (3) shows a minimum and corresponds to a nearly monodisperse system of spheres with σ_a = 0.05. Subtracting this curve from the measured one, we got the scattering curve in Fig. 13c, which could be fitted excellently by a model curve with σ_a = 0.1. Assuming the same structural density for both components one can calculate their mass fractions by the expression:

$$\mathbf{M^*_{w1} / M^*_{w2} = x_1 M_{w1} /(1 - x_1) M_{w2} = (x_1 /(1 - x_1))(a_{m1} / a_{m2})^3} \qquad (25)$$

where $\mathbf{M^*_{wi}}$ are the products of the masses times the mass fractions of the components, obtained after the curve separation. The structural parameters of both components are collected with the values of the PEC at 25 °C in Table 2.

Table 2. Structural parameters of the PEC AIFL/2AIFL3 in 0.025 N NaCl at 25 and 50 °C.

T (°C)	σ_a	M_w^* g/mol	M_w g/mol	x_i	a_m (nm)	ρ g/ml
25	0.2		$1.80\ 10^9$	1	178	0.13
50	0.1	$2.28\ 10^9$	$2.56\ 10^9$	0.89	118	0.62
50	0.05	$2.64\ 10^9$	$2.40\ 10^{10}$	0.11	248	0.62

It should be emphasized that the detailed analysis of one scattering curve provided in an accurate manner all parameters of the bimodal system. The swelling- deswelling behavior is once more the decisive effect.

Conclusions

Summarizing all results obtained, the following structure model can be proposed:

The PEC particles consist of a neutralized compact core and a surrounding shell of the excess component. The level of aggregation reaches up to several thousand chains and is mainly controlled by the concentration of the component solutions and the ionic strength during complex formation. The compactness of the core can be varied via the charge densities of the components. At non-stoichiometric mixing ratios the excess component stabilizes the neutralized core with regard to secondary aggregation.

Depending on the nature of the components subsequent addition of salt may cause secondary aggregation and finally flocculation, but also complete dissolution of the PECs at a critical salt concentration. PECs between temperature-sensitive polyelectrolytes show a temperature-controlled swelling behavior. PEC particles should be of general interest as carrier systems for drugs and biological objects.

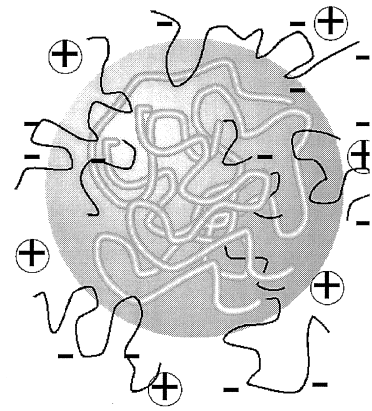

References

1. E. Tsuchida, Y. Osada, K.Samada, *J. Polym. Sci . A1*, **10**, 3397 (1972)
2. E.Tsuchida, Y. Osada, H. Ohno, *Macrom. Sci.* **B17**, 683 (1980)
3. V. A. Kabanov, in: Macromolecular Complexes in Chemistry and Biology, ed. by P. Dubin et al., Springer Verlag Berlin, New York 1994, Chapter 10, 151.
4. V. A. Kabanov, A. B. Zezin, *Makromol. Chem. Suppl.* **10,** 259 (1984)
5. K. N. Bakeev, V. A. Izumrudov, A. B. Zezin, V. A. Kabanov, *Dokladi Akad. Nauk* **299**, 1405 (1988)
6. B. Philipp, H. Dautzenberg, K.J. Linow, J. Koetz, W. Dawydoff, *Prog. Polym. Sci.*, **14**, 91 (1989)
7. F. Brand, H. Dautzenberg, W. Jaeger, M. Hahn, *Appl. Macromol. Chem.* **248**, 41 (1997)
8. M. Hahn, E. Görnitz, H. Dautzenberg, *Macromolecules* **31**, 17, 5616 (1998)
9. H. Dautzenberg, G. Rother, *J. Polym. Sci., Polym. Phys. Ed., Part B* **76,** 353 (1988)
10. M. Kerker: The Scattering of Light and other Electromagnetic Radiation, Academic Press, New York 1969
11. H. Dautzenberg, G. Rother, *Makromol. Chem., Macromol. Symp.* **61**, 94 (1992)
12. B.Chu : Laser Light Scattering, Second Edition, Academic Press 1991
13. K.S. Schmitz: Dynamic Light Scattering by Macromolecules, Academic Press, San Diego 1990
14. S. W. Provencher, *Comp. Phys. Comm.* **27,** 213 (1982)
15. H. Dautzenberg, G. Rother, J. Hartmann, in: ACS Symposium Series 548: Macro-ion Characterization, ed. by K. S. Schmitz, American Chemical Society, Washington, DC, 1994, Chapter 16, 220
16. H.Dautzenberg, J. Hartmann, S. Grunewald, F. Brand, *Ber. Bunsen-Gesellschaft, Conference Proceedings of "Polyelectrolytes Potsdam' 95"* **100**,6, 1024 (1996)
17. K.-H. Wassner, U. Schroeder, D. Horn, *Makromol. Chem.* **192**, 553 (1991)
18. G. S. Manning, *J. Chem. Phys.* **51**, 924 (1969)
19. F. Brand, H. Dautzenberg, *Langmuir* **13**, 11, 2905 (1997)
20. N. Karibyants, H. Dautzenberg, H.Cölfen, *Macromolecules* **30**, 25, 7803 (1997)
21. G. Schmal, D. Rudolph, P. Guttmann, J. Thieme, G. Schneider, C. David, M. Diehl, T. Wilhelm, *Optik* **93**, 95 (1993)
22. H. Dautzenberg, *Macromolecules* **30**, 25, 7810 (1997)

23. H. Dautzenberg, N. Karibyants, *Macromol. Chem. Phys.* **200**, 118 (1998)

Acknowledgement

I thank U. Lück and B. Schonert for careful technical assistance as well as Dr. G. Rother, Dr. F.Brand, Dr. N. Karibyants, Dr. J. Hartmann, and Dr. H. Cölfen for fruitful cooperation. The financial support of the Deutsche Forschungsgemeinschaft is gratefully acknowledged.